IIETA International Information and Engineering Technology Association
Advancing the World of Information and Engineering

Mathematical Modelling of Engineering Problems
Vol. 11, No. 10, October, 2024, pp. 2749-2762
Journal homepage: http://iieta.org/journals/mmep

Optimization Acceleration and Contact Force of Space Slider-Crank Mechanism with Spherical Clearance Joints

Minh Hung Vu[1], Phan Anh Nguyen[1], Ngoc Thai Huynh[2*], Tien Phuoc Le[3], Quoc Manh Nguyen[4], Nguyen Ho[5]

[1] Faculty of Fundamental Sciences, PetroVietnam University, Ba Ria 790000, Vietnam
[2] Faculty of Mechanical Engineering Technology, Ho Chi Minh City University of Industry and Trade, Ho Chi Minh City 700000, Vietnam
[3] Faculty of Automotive, Ho Chi Minh City Industry and Trade College, Ho Chi Minh City 700000, Vietnam
[4] Faculty of Mechanical Engineering, Hung Yen University of Technology and Education, Khoai Chau 160000, Vietnam
[5] Faculty of Electrical and Electronics Engineering, Ton Duc Thang University, Ho Chi Minh City 700000, Vietnam

Corresponding Author Email: thaihn@huit.edu.vn

https://doi.org/10.18280/mmep.111017

Received: 29 March 2024
Revised: 2 July 2024
Accepted: 15 July 2024
Available online: 31 October 2024

Keywords:
grey relational analysis, Taguchi method, TOPSIS method, SAW method, WAPAS method, Runge-Kutta 4, ANSYS

ABSTRACT

Clearance always exists in revolute kinematic joints and spherical joints due to manufacturing, assembly, wear, etc., Proper clearance helps the mechanism operate smoothly. However, the friction inside the joint causes the joint clearance to increase, resulting in mechanical vibrations. These are demonstrated through the analysis of the dynamics of the spatial slider crank mechanism using Rigid dynamics. in ANSYS. To ensure smooth operation of the space slider crank mechanism. It is necessary to select the length of the crank, the revolute and ball joint clearances, the friction coefficient inside the kinematic joint and the crank driving speed. Because these design parameters all affect the slider acceleration and the contact force within revolute and clearance ball joints. To do this, the Grey-Taguchi method is proposed. From the results of the rigid dynamics analysis of the spatial slider crank mechanism, it has been proven that increasing the design variables causes the acceleration and contact force to increase significantly, causing instability for the crank mechanism. space slider. The grey relational analysis -Taguchi optimization results also confirm this. The results of grey relational Analysis-Taguchi method achieved the optimal acceleration of the slider and the optimal contact force in the revolute joint of the space slider crank mechanism being 32.72 m/s^2 and 1.3452 kN, respectively. To increase the reliability of this optimization method, decision-making methods with multiple criteria or multiple objectives are also applied, such as the TOPSIS method, the SAW method and the WASPAS method. The results of these methods confirm the same results as the Grey-Taguchi method. The optimal results were chosen the space slider crank mechanism model with crank size, friction coefficient, revolute joint and ball joint clearance sizes and crank driving speed 80 mm, 0.01, 0.1 mm and 800 rpm, respectively.

1. INTRODUCTION

The clearance in traditional joints not only helps the link joints move easily but also affects the workability of the mechanical system, such as wear due to friction and the noise caused by vibration due to impact. To reduce the influence of dry friction inside the joint with clearance, lubrication for multiple joints with clearance was studied and the dynamic model of the multi-joint planar mechanism with clearance is constructed based on the dynamic accuracy reliability model and the Lagrange multiplier method for the 2DOF mechanism with 9 links [1]. The clearance model of the through-joint and the forward-joint is used to establish the dynamic equation of the 6-bar planar mechanism based on the Lagrange multiplier method [2]. This model is further confirmed by ADAM and experimentally. The Baumgarte method was used to improve the oscillation of the slider-crank mechanism caused by the translational and revolute clearances. The accuracy of the model was evaluated experimentally [3]. The experimental results also showed that the revolute clearance caused more oscillation than the translational clearance. The contact force model and the internal wear model in a rotary joint with clearance are proposed to determine the wear amount by the non-contact method. A contact force model and an internal wear model in a rotary joint with clearance are proposed to determine the wear amount by a non-contact method [4]. The measured results are compared with the numerical simulation results. The extended alpha method is based on Newton's collision law to describe the dynamic model of a spherical joint with clearance [5]. This method can avoid singularities and invariances. The time method is also used to determine the results of the alpha method. The effects of curvature radius of

asperities contact speed, and roughness on dynamic response of rudder loop with revolute joint clearance were determined the Lagrange method [6]. The outcomes identified that when clearance size increased and impacted frequency nonlinearly increased, rudder angle error and contact force increased. The finite particle method is proposed to determine the influence of internal friction in revolute joints with clearance [7]. The proposed model determines that as the clearance size increases, the mechanism oscillates more strongly. As the friction coefficient increases, the oscillation of the mechanism decreases, and as the damping coefficient increases, the energy dissipation increases significantly. The fuzzy sets and fuzzy algorithms were utilized to determine the influence of clearance tolerance on the dynamic behavior of the mechanism [8]. The contact force model was applied to determine the internal contact force in the effective clearance rotary joint for small clearance sizes. The center of curvature method is applied to determine the effect of non-circular joints with clearance on the dynamic behavior of the mechanism [9]. Simulation results confirm that the center of curvature model achieves the dynamic behavior of the multi-body mechanism similar to the traditional geometric center method. The flexibility of the mechanism significantly affected the dynamic behavior of the slider-crank mechanism [10]. The Lagrange multiplier technology [11] was applied to develop a dynamic model of a mechanism with three spherical joints. The results of this model indicate that as the gap size increases the dynamic behavior of the mechanism oscillates chaotically. ADAMS and MATLAB were used to validate the results. The edited friction force model and innovated nonlinear impact force model were applied to investigate the dynamic behavior of a planar mechanical system [12]; the models were then experimentally validated. The influences of clearance size and input velocity on the dynamic response of the slider-crank mechanism were estimated by the nonlinear continuous contact force model and flexible link [13]. The revised Coulomb's friction law and Archard's wear law were applied to investigate a rigid-flexible coupling system's dynamic behavior and wear with clearance joints based on the NCF-ANCF formulation [14]. The influences of the clearance size and the cylinder stiffness were analyzed by a modified CF model and LuGre model [15]. The experiment was carried out to validate the effectiveness of the proposed method, as well as to demonstrate a new method to construct the manipulator, which has high computational efficiency and accurately. A dynamic equation with a Lagrange multiplier was established for the spherical clearance joints of the parallel spatial mechanism [16]. The effects of one clearance joint were approximated for the case of an ideal joint. The dynamic behavior of a mechanical system is more strongly affected than those with one clearance joint and an ideal joint. The clearance and the branched-chain elasticity introduced errors to the robot motion, which was investigated by the rigid–flexible coupling dynamic model having clearance and the spatial beam element. The wear of the spherical clearance joint was investigated [17] by the Archard wear model. The edited Flores CF model and the modified Coulomb friction model using the Newton-Euler method, and the 4^{th}-order Runge-Kutta method were applied to analyze the dynamic model of the parallel mechanism with the spherical clearance joint [18]. The effects of the clearance joint on the wear of the mechanical systems [19] were confirmed by Archard's theory and Coulomb's model. The contact collision model, friction model and the modified Coulomb friction model [20] were applied to investigate the effect of friction in the clearance joint. The transfer matrix method was applied to determine the effects of the RCJ on the rigid-flexible coupling multi-link dynamics model. The influences of clearance size on the translation clearance joint and driven speed of the slider-crank mechanism were investigated [21] using the LuGre friction model and the modified L-N contact model. Analysis of design variable on rigid and flexible dynamics of space slider crank mechanism [22]. A grey relational analysis based Taguchi method [23] was utilized to optimize dynamic of space slider-crank mechanism and the stress in the flexible connecting rod. The optimal results were verified by TOPSIS method. The spherical clearance joint model, contact force model and spherical clearance joint lubrication model [24] has been established to describe the dynamics of multi-body systems with spherical joints. The simulation results indicated that spherical clearance joint lubrication model took simulation much more time than the other. In order to reduce the effects of contact force are due to friction causes. Therefore, the improvement lubrication model in spherical clearance joint [25] proposed. The simulation results identified that the effects of clearance size and friction on the acceleration significantly reduced. The effects of the clearance size and friction in spherical clearance joint and revolute clearance joint were analyzed by the Lagrange multiplier technique and Jacobian of constraint matrix [26] and were confirmed by ADAMS and Newton–Euler method.

The novel in this investigation identified as following:

•The model of space slider crank mechanism in this investigation was designed to reduce the weight and was optimized the effects of the design variables on the acceleration of the slider and the contact force in the revolute clearance joint. While the reference [22] only analyzed the effect of the design variable.

•The design model of the space slider crank mechanism in reference [23] designed the working length of the slider to be large. Because the crank was designed in the plane made with the horizontal plan of 135 degrees. While the design model of the investigation, the working length of the slider is lower. Because the crank was designed in the plane made with the horizontal plan of 90 degrees.

•The Runge-Kutta 4 rigid dynamics model in ANSYS, the grey relational analysis based on the Taguchi method [27], and the TOPSIS, WASPAS methods [28] and SAW method [29], and were used to estimate and reduce the influences of clearance size in the revolute and spherical joints with clearance and friction on the dynamic behavior of the space slider-crank mechanism. Other models, such as the analysis of variance, analysis of means, and analysis of the interaction of the design variables, were also applied to verify the design variable influence on the acceleration of the slider and the CF in the RCJ and spherical clearance joints.

•Previous studies mostly used the Lagrange equation or Neton's 2nd law to model and establish the differential equation of motion of the system and used the programming language MATLAB or Fortran to solve this system of equations. This is an effective method. However, this method requires the researcher to be proficient in using programming language to solve the problem. For researchers who do not know how to use programming languages, solving is very difficult. Different from the previous study, in this study, it is proposed to analyze and simulate the dynamics of the mechanical system using ANSYS and the optimization is

performed using grey relational analysis methods - Taguchi method, TOPSIS method, SAW method, WASPAS method.

The remaining of the investigation was written as following: The clearance model in the revolute and spherical joints, the mechanism model, the Runge-Kutta 4 model, and the MEREC method are presented in Section 2. The grey relational analysis based on the Taguchi method and the TOPSIS, SAW, and WASPAS methods are presented in Section 3. The results are discussed in Section 4, and the conclusions are presented in Section 5.

2. DESIGN OF THE SPACE SLIDER CRANK MECHANISM AND SIMULATION

2.1 Mechanism model and configuration in ANSYS

The space slider-crank mechanism, depicted in Figure 1, was created in SolidWorks and analyzed by the Runge-Kutta 4 rigid dynamics model in ANSYS as presented in Table 1. The model consists of the following links: the base is the first link, the crank is the second link, the connecting rod is the third link, and the slider is the fourth link.

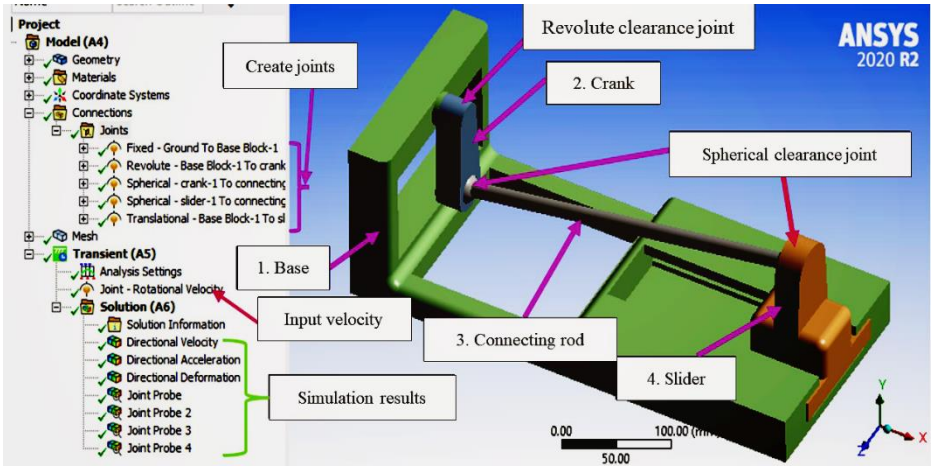

Figure 1. Space slider-crank mechanism model

Table 1. Set up initial condition and select time integration type

Step Control	
Number of Steps	1
Current Step Number	2s
Auto Time Stepping	off
Time Step	0.001s
Solver Control	
Time Integration Type	Runge-Kutta 4
Correction Type	With Inertia Matrix
Assembly Type	Pure Kinematic
Nonlinear Control	
Energy Accuracy Toler…	Program Controlled
Output Control	
Store Results at	All Time Points
Analysis Data Management	
Solver Files Directory	E:\3D-SILDER-FLEXIBLE\1_fil..
Scratch Solver Files Di…	
Visibility	
[A] Joint-Rotational…	Display

In the plane slider-crank mechanism, all points on the moving link move in planes parallel to each other, the slider runs in a direction perpendicular to the centreline of the crank's bearing. The space slider-crank mechanism is not subject to the above constraints, so it is very diverse. According to the coordinate system as shown in Figure 1, the space slider crank mechanism works according to the principle: first the crank rotates around the x axis in the YOZ plane and is driven by hand or by a motor that transmits motion through the connecting rod. The first spherical joint with clearance was utilized to link between crank and connecting rod. Next, the rotating connecting rod transmits motion through the slider thanks to the second spherical joint with clearance. This causes the linear motion slider along the x axis in the XOZ plane. This principle puts the rotational motion of the crank into the translational motion of the slider. This mechanism has many widespread applications in industry such as presses, aircraft wheel folding mechanisms, hydraulic cylinders.

The Runge-Kutta 4 model in ANSYS was utilized to determine the velocity and acceleration of the slider as well as the CF in the spherical joints and the RCJ. The simulation parameters are listed in Table 2.

Table 2. Dimensions and weights of the links

Parameters	Value
Crank length (mm)	80, 100 and 120
Crank mass (kg)	0.72009
Connecting rod length (mm)	350
Connecting rod mass (kg)	0.5166
Slider mass (kg)	3.5826

Structural steel was used for all the links in the model with a modulus of elasticity of 200 GPa, Poisson's ratio of 0.3, and density of 7850 kg/m^3. The model of the meshed divide was automatically used for dividing the mesh of a model with four elements and four nodes. The fixed joint was set as the first link, the revolute joint was configured to connect the first link and the second link, the first spherical joint was configured to connect the second link and the third link, and the translation joint was configured to connect the third link and the fourth link. The journal's and bearing's initial centers were concentric, and the ball's and socket's centers were concentric, with a time step of 0.001 seconds. The values of four design parameters were varied to perform 27 simulation cases: crank lengths (80 mm, 100 mm, and 120 mm); driven speeds (800

rpm, 1000 rpm, and 1200 rpm); friction coefficient (0.01, 0.05, and 0.1); and clearance size (0.1 mm, 0.4 mm, and 0.7 mm).

2.2 RCJ model

The RCJ model is shown in Figure 2 [30-35]. The clearance size was determined by the bearing radius minus the axle radius and is written in Eq. (1).

$$c = r_B - r_j \tag{1}$$

where r_B and r_j are the bearing radius and the axle radius, respectively, and d_B are the bearing length and the bearing diameter, respectively.

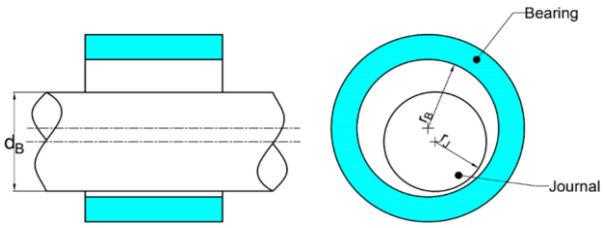

Figure 2. Revolute clearance axle model [35]

2.3 SCJ model

The SCJ model [16, 18, 22-26] is illustrated in Figure 3. The clearance size in the spherical joint was determined by the socket radius minus the ball radius.

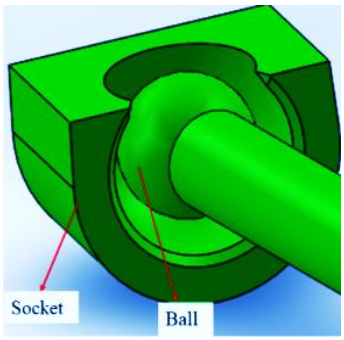

Figure 3. Spherical clearance joint model

2.4 Estimating the weight by MEREC method

To obtain the weight of each output, MEREC method [36-39] is applied and is implemented:

Step 1: Determine the target

The target: "The largest value is the best".

$$h_{ij} = \frac{\min a_{ij}}{a_{ij}} \tag{2}$$

The target: "The smallest value is the best."

$$h_{ij} = \frac{a_{ij}}{\max a_{ij}} \tag{3}$$

where, a_{ij} are the output values. u_{ij} are the acceleration and CF. The values are archived by the Runge-Kutta 4 rigid dynamics model in ANSYS.

Step 2: Determine the total performance of the criteria

$$S_i = \ln\left[1+\left(\frac{1}{n}\sum_{j}^{n}\left|\ln\left(h_{ij}\right)\right|\right)\right] \tag{4}$$

Step 3: Determine the performance of the criteria

$$S_{ij}^{'} = \ln\left[1+\left(\frac{1}{n}\sum_{k,k\neq j}^{n}\left|\ln\left(h_{ij}\right)\right|\right)\right] \tag{5}$$

Step 4: Determine the deviation

$$E_j = \left|S_{ij}^{'} - S_i\right| \tag{6}$$

Step 5: Determine the weight of every criterion

$$w_k = \frac{E_j}{\sum_{k}^{m} E_k} \tag{7}$$

3. OPTIMIZATION METHOD

3.1 Grey relational analysis

In order to achieve the optimal solution, the smallest acceleration and contact force is best. This is a multi-objective problem that cannot be achieved with the Taguchi method. Therefore, grey relational analysis [27, 40-44], is applied and performed as follows. Firstly, the design variables were selected. After, 27 models were designed by SolidWorks based on the design of experiment result of Minitab software. Finally, acceleration and contact force are recorded from the results of dynamic analysis:

Step 1: Determine the target:

The target: "The largest value is the best."

$$D_i^* = \frac{D_i^{(0)}(k) - \min D_i^0(k)}{\max D_i^{(0)}(k) - \min D_i^{(0)}(k)} \tag{8}$$

The target: "The smallest value is the best."

$$D_i^* = \frac{\max D_i^{(0)}(k) - D_i^0(k)}{\max D_i^{(0)}(k) - \min D_i^{(0)}(k)} \tag{9}$$

where, $D_i^{(0)}(k)$ are the output values. $D_i^{(0)}(k)$ are the acceleration and CF which were obtained by the Runge-Kutta 4 rigid dynamics model in ANSYS.

Step 2: Calculation deviation:

$$\Delta_{0i} = \left\|D_0^*(k) - D_i^*(k)\right\| \tag{10}$$

$$\Delta_{\min} = \max_{\forall j\in i} \min_{\forall k} \left\|D_0^*(k) - D_j^*(k)\right\| \tag{11}$$

$$\Delta_{\max} = \max_{\forall j\in i} \max_{\forall k} \left\|D_0^*(k) - D_j^*(k)\right\| \tag{12}$$

Step 3: Estimate the grey relational coefficient (GRC) (γ) as follows:

$$\gamma_i(k) = \frac{\Delta_{\min} + \xi\Delta_{\max}}{\Delta_{0i} + \xi\Delta_{\max}} \tag{13}$$

where, $\xi \in [0,1]$ is the distinguishing coefficient, typically with a value of 0.5.

Step 4: Compute GRG (ψ_i) as follows:

$$\psi_i = \sum_{k=1}^{n} w_k \gamma_i(k) \tag{14}$$

where, n=27, where w_k is determined in Section 2.4.

Step 5: Determine the maximum value of GRG as the optimal value. The case where this maximum value is achieved is the optimal case.

The signal to noise ratio obtained by "the maximum value is better" [45-48]:

$$S/N = -10\log\left(\frac{1}{n}\sum_{i=1}^{n}\frac{1}{y_i^2}\right) \tag{15}$$

where, y_i is GRG values:

Determine the forecasted value of GRG:

$$\mu_G = G_m + \sum_{i=1}^{q}(G_0 - G_m) \tag{16}$$

Compute CI value at $\alpha = 0.05$ by employing Eq. (17):

$$CI_{CE} = \pm\sqrt{F_\alpha(1, fe)Ve\left(\frac{1}{n_{eff}} + \frac{1}{R_e}\right)} \tag{17}$$

The $F_\alpha(1, fe)$ was obtained from Table B-2 in reference [49].

3.2 TOPSIS method

The decision-making method based on multiple criteria is the technique for order preference by similarity to ideal solution (TOPSIS) invented in 1980. This method helps select an optimal model based on many criteria such as the required slider speed being small, the contact force inside the rotary joint and ball joint of the system must be small, and the system must be durable enough. With different model sizes, different criteria are achieved. It is necessary to determine an optimal model with many criteria or multiple goals. To achieve the desired advantages, the TOPSIS method is very useful in this. In order the optimal case, the TOPSIS method [28, 50-54] is utilized and is implemented:

Step 1: Determine the normalized values of the objective

$$n_{ij} = \frac{a_{ij}}{\sqrt{\sum_{i=1}^{n} a_{ij}^2}} \tag{18}$$

where, a_{ij} the acceleration and CF archived by the Runge-Kutta 4 rigid dynamics model in ANSYS.

Step 2: Determine the weighted normalized values of the acceleration and CF

$$v_{ij} = w_k n_{ij} \tag{19}$$

where, w_k is determined in Section 2.4.

Step 3: Determine the biggest and smallest of b_{ij}

$$b^+ = \left(b_1^+, b_2^+, \ldots b_n^+\right) \tag{20}$$

$$b^- = \left(b_1^-, b_2^-, \ldots b_n^-\right) \tag{21}$$

Step 4: Determine the values S_i^+ and S_i^- of the optimal criteria

$$S_i^+ = \sqrt{\sum_{j=1}^{n}\left(b_{ij} - b_j^+\right)^2} \tag{22}$$

$$S_i^- = \sqrt{\sum_{j=1}^{n}\left(b_{ij} - b_j^-\right)^2} \tag{23}$$

Step 5: Determine the values for CC_i

$$CC_i = \frac{S_i^-}{S_i^+ + S_i^-} \tag{24}$$

Step 6: Determine the biggest value of CC_i as the optimal values. The case where this maximum value is achieved is the optimal case.

3.3 SAW method

In order to increase the reliability of the Grey-Taguchi and TOPSIS methods, the SAW (Simple Additive Weighting) Method commonly used in decision making for multi-objective problems [52] and was carried out step by step:

Step 1: Determine the normalized values of every criterion

The target: "The largest value is the best."

$$n_{ij} = \frac{a_{ij}}{\max a_{ij}} \tag{25}$$

$$n_{ij} = \frac{\min u_{ij}}{u_{ij}} \tag{26}$$

where, a_{ij} the acceleration and CF which are archived by the Runge-Kutta 4 rigid dynamics model in ANSYS.

Step 2: Determine the sum of the weight normalized values

$$v_i = \sum_{j=1}^{n} w_k \cdot n_{ij} \tag{27}$$

where, w_k is determined in Section 2.4.

Step 3: Determine the biggest value v_i as the optimal value. The case where this maximum value is achieved is the optimal case.

3.4 WASPAS method

Besides, optimum results were also performed using the WASPAS method [28, 49, 55, 56]. WASPAS is also one of the most effective decision-making methods for selecting the optimal case that meets multiple criteria or multiple objectives, was performed as follows:

Step 1: Using Eq. (25) and Eq. (26) to determine n_{ij}, next determine v_{ij}, Q_i, and P_i.

$$v_{ij} = w_k \cdot n_{ij} \tag{28}$$

where, w_k is determined in Section 2.4.

$$Q_i = \sum_{j=1}^{n} v_{ij} \tag{29}$$

$$Q_i = \sum_{j=1}^{n} v_{ij} P_i = \prod_{j=1}^{n} \left(v_{ij}\right)^{w_i} \tag{30}$$

Step 2: Determine A_i

$$A_i = \lambda \cdot Q_i + (1-\lambda) \cdot P_i, \lambda = 0.9 \tag{31}$$

Step 3: Determine biggest value A_i as the optimal value. The case where this maximum value is achieved is the optimal case.

The acceleration and CF which are two criteria that need to be achieved when designing a space slider crank mechanism with design variables being crank length, clearance size, coefficient friction and input velocity. The optimal case is selected as the highest value of the grey relational grade, and the optimal result of the Grey-Taguchi method is determined by the TOPSIS method, SAW method and WASPAS method. Applying the Taguchi method by performing 27 cases is relatively sufficient to determine the optimal case.

4. RESULTS AND DISCUSSION

4.1 Design simulation

In order to minimize the CF and acceleration, it is necessary to obtain the optimal values for the design variables. The 27 experimental cases were established using Minitab 18 software, with the design variables highlighted in Table 3. In this table, the first variable is crank length and is symbolled by x with three level 80 mm, 100 mm and 120 mm, the second variable is clearance size and is symbolled by y with three level 0.1 mm, 0.4 mm and 0.7 mm, the third variable is coefficient friction and is symbolled by z with three level 0.01, 0.05 and 0.1, the fourth variable is input velocity and is symbolled by t with three level 800 rpm, 1000 rpm and 1200 rpm. The values for the acceleration of the slider and CF were calculated from the 27 experimental cases, as presented in Table 4. As can be seen in the table, increasing crank length significantly increases the acceleration and CF. Similarly, increasing clearance size and friction coefficient increases the acceleration and CF slightly. However, the input velocity significantly affects acceleration and CF.

Table 3. Design variables and their level

Factor	Symbol	Unit	Levels		
			1	2	3
Crank length	x	mm	80	100	120
Clearance size	y	mm	0.1	0.4	0.7
Coefficient friction	z		0.01	0.05	0.1
Input velocity	t	rpm	800	1000	1200

Table 4. The L_{27} orthogonal array and simulation results

Trial No.	Crank Length (mm)	Clearance Size (mm)	Coefficient Friction	Input Velocity (m/s)	Acceleration (m/s^2)	CF (KN)
1	80	0.1	0.01	800	32.72	1.3452
2	80	0.1	0.05	1000	51.128	1.7555
3	80	0.1	0.1	1200	73.624	1.9552
4	80	0.4	0.01	1000	41.157	1.594
5	80	0.4	0.05	1200	62.67	1.7622
6	80	0.4	0.1	800	70.799	1.0611
7	80	0.7	0.01	1200	50.666	1.6565
8	80	0.7	0.05	800	54.741	1.0114
9	80	0.7	0.1	1000	80.158	1.1767
10	100	0.1	0.01	800	52.498	1.2356
11	100	0.1	0.05	1000	66.842	2.0509
12	100	0.1	0.1	1200	83.371	3.0839
13	100	0.4	0.01	1000	62.803	2.151
14	100	0.4	0.05	1200	76.316	2.9921
15	100	0.4	0.1	800	79.471	3.1202
16	100	0.7	0.01	1200	72.147	2.9518
17	100	0.7	0.05	800	70.399	2.9368
18	100	0.7	0.1	1000	87.684	4.0212
19	120	0.1	0.01	800	93.69	4.6123
20	120	0.1	0.05	1000	100.9	5.9118
21	120	0.1	0.1	1200	110.83	7.5641
22	120	0.4	0.01	1000	103.06	6.4221
23	120	0.4	0.05	1200	110.04	7.8202
24	120	0.4	0.1	800	106.8	8.6251
25	120	0.7	0.01	1200	112.74	8.0592
26	120	0.7	0.05	800	105.54	8.6719
27	120	0.7	0.1	1000	114.23	10.4971

Table 5. Results of the weight determination method

Experiment No.	h_{ij}		S_i	$b_{ij'}$		E_j	
	D_i	S_t		D_i	S_t	D_i	S_t
1	0.2864	0.1281	0.9755	0.4856	0.7067	0.4899	0.2211
2	0.4476	0.1672	0.8312	0.3379	0.6388	0.4934	0.3009
3	0.6445	0.1863	0.7227	0.1985	0.6099	0.5241	0.4114
4	0.3603	0.1519	0.8972	0.4124	0.6639	0.4849	0.2516
5	0.5486	0.1679	0.7850	0.2625	0.6378	0.5225	0.3753
6	0.6198	0.1011	0.8692	0.2145	0.7636	0.6548	0.5491
7	0.4435	0.1578	0.8457	0.3411	0.6540	0.5046	0.3129
8	0.4792	0.0964	0.9313	0.3132	0.7747	0.6180	0.4615
9	0.7017	0.1121	0.8204	0.1631	0.7392	0.6573	0.5761
10	0.4596	0.1177	0.8995	0.3284	0.7274	0.5712	0.3991
11	0.5852	0.1954	0.7345	0.2374	0.5969	0.4971	0.3595
12	0.7299	0.2938	0.5709	0.1462	0.4778	0.4247	0.3315
13	0.5498	0.2049	0.7380	0.2617	0.5837	0.4763	0.3220
14	0.6681	0.2850	0.6039	0.1837	0.4871	0.4202	0.3034
15	0.6957	0.2972	0.5811	0.1667	0.4741	0.4144	0.3074
16	0.6316	0.2812	0.6228	0.2068	0.4912	0.4160	0.2844
17	0.6163	0.2798	0.6307	0.2167	0.4928	0.4140	0.2761
18	0.7676	0.3831	0.4775	0.1242	0.3919	0.3533	0.2677
19	0.8202	0.4394	0.4123	0.0945	0.3444	0.3178	0.2499
20	0.8833	0.5632	0.2994	0.0602	0.2524	0.2393	0.1922
21	0.9702	0.7206	0.1646	0.0150	0.1517	0.1496	0.1367
22	0.9022	0.6118	0.2602	0.0502	0.2197	0.2100	0.1695
23	0.9633	0.7450	0.1535	0.0185	0.1373	0.1350	0.1188
24	0.9350	0.8217	0.1238	0.0331	0.0937	0.0908	0.0606
25	0.9870	0.7678	0.1299	0.0065	0.1241	0.1234	0.1176
26	0.9239	0.8261	0.1267	0.0388	0.0912	0.0879	0.0524
27	1.0000	1.0000	0.0000	0.0000	0.0000	0.0000	0.0000

Table 6. Grey relational analysis and GRG rank

Experiment No.	$D_i^*(1)$	$D_i^*(2)$	$\Delta_{oi}(1)$	$\Delta_{oi}(2)$	$\gamma_i(1)$	$\gamma_i(2)$	ψ_i	Rank
1	1.0000	0.9650	0.0000	0.0350	1.0000	0.9346	0.9726	1
2	0.7740	0.9220	0.2260	0.0780	0.6887	0.8651	0.7625	6
3	0.4980	0.9010	0.5020	0.0990	0.4990	0.8347	0.6395	12
4	0.8960	0.9390	0.1040	0.0610	0.8278	0.8913	0.8544	2
5	0.6330	0.9210	0.3670	0.0790	0.5767	0.8636	0.6968	8
6	0.5330	0.9950	0.4670	0.0050	0.5171	0.9901	0.7151	7
7	0.7800	0.9320	0.2200	0.0680	0.6944	0.8803	0.7722	5
8	0.7300	1.0000	0.2700	0.0000	0.6494	1.0000	0.7962	3
9	0.4180	0.9830	0.5820	0.0170	0.4621	0.9671	0.6735	9
10	0.7570	0.9760	0.2430	0.0240	0.6729	0.9542	0.7907	4
11	0.5810	0.8900	0.4190	0.1100	0.5441	0.8197	0.6595	11
12	0.3790	0.7820	0.6210	0.2180	0.4460	0.6964	0.5508	17
13	0.6310	0.8800	0.3690	0.1200	0.5754	0.8065	0.6721	10
14	0.4650	0.7910	0.5350	0.2090	0.4831	0.7052	0.5761	15
15	0.4260	0.7780	0.5740	0.2220	0.4655	0.6925	0.5605	16
16	0.5160	0.7950	0.4840	0.2050	0.5081	0.7092	0.5923	14
17	0.5380	0.7970	0.4620	0.2030	0.5198	0.7112	0.5999	13
18	0.3260	0.6830	0.6740	0.3170	0.4259	0.6120	0.5038	18
19	0.2520	0.6200	0.7480	0.3800	0.4006	0.5682	0.4708	19
20	0.1640	0.4830	0.8360	0.5170	0.3743	0.4916	0.4234	20
21	0.0420	0.3090	0.9580	0.6910	0.3429	0.4198	0.3751	22
22	0.1370	0.4300	0.8630	0.5700	0.3668	0.4673	0.4089	21
23	0.0510	0.2820	0.9490	0.7180	0.3451	0.4105	0.3725	23
24	0.0910	0.1970	0.9090	0.8030	0.3549	0.3837	0.3670	25
25	0.0180	0.2570	0.9820	0.7430	0.3374	0.4023	0.3646	26
26	0.1070	0.1920	0.8930	0.8080	0.3589	0.3823	0.3687	24
27	0.0000	0.0000	1.0000	1.0000	0.3333	0.3333	0.3333	27

4.2 Results of the weight determination method

The outcomes of Eqs. (3)-(6) as listed by Table 5. The weight of the acceleration and CF obtained by Eq. (7) are 0.5814 and 0.4186, respectively.

4.3 Grey relational analysis

The results of GRA are listed in Table 6. The values of the objective functions $D_1^*(1)$, $D_1^*(2)$ were determined by Eq. (9) with the values of the acceleration of the slider and contact force. The deviation values $\Delta oi(1)$, $\Delta oi(2)$ were determined by

Eq. (10). The GRC ($\gamma_i(1)$, $\gamma_i(2)$) were obtained by Eq. (13). The GRG (ψ_i) were obtained by Eq. (14). The rank values were determined by ranking the GRG. The maximum value for GRG was determined by the first rank; thereby, the case ranked as one is considered the optimal case. The simulation results of 27 cases obtained with the different values of GRG indicated that the design variable have affected on the acceleration and CF. The problem consistent with previous studies [2, 5-7, 23, 24]. This means the acceleration and the contact force depend on the crank length, clearance size, coefficient friction and input velocity.

4.4 Analysis of signal to noise (S/N)

The values of the S/N average of the design variables thereby every level was listed in Table 7. The delta is computed by the values of Level 1 minus Level 3. The values in the table reveal that the maximum values are the optimal cases for the design variables. The rank of 1 indicates that variable (x) strongly effected on the acceleration and CF; next is variable (z), variable (t), and finally, variable (y). The data in this table were also used to create the graph shown in Figure 4. The effect of the level of the design variables was verified by applying the Taguchi Method based on the analysis of S/N, as shown Figure 4. The levels of the design variables are listed horizontally, with the S/N values presented vertically. The high peak on the graph indicates that at the position obtained, the optimal levels of the design variables were $x_1 y_1 z_1 t_1$. The larger the slope, the stronger the influence of those variables on the GRG values. The variable (x) therefore, has a significant influence on the acceleration of the slider and CF in the revolute clearance joint and spherical joints, followed by the variable (z), variable (t), and finally, variable (y). The problem consistent with previous studies [2, 5-7, 23, 24]. This means the acceleration and the CF depend on the crank length, clearance size, coefficient friction and input velocity.

Table 7. Values of S/N of GRG

Level	x	y	z	t
1	-2.139	-4.208	-3.942	-4.299
2	-4.069	-4.862	-4.787	-4.781
3	-8.157	-5.295	-5.636	-5.285
Delta	6.018	1.087	1.694	0.986
Rank	1	3	2	4

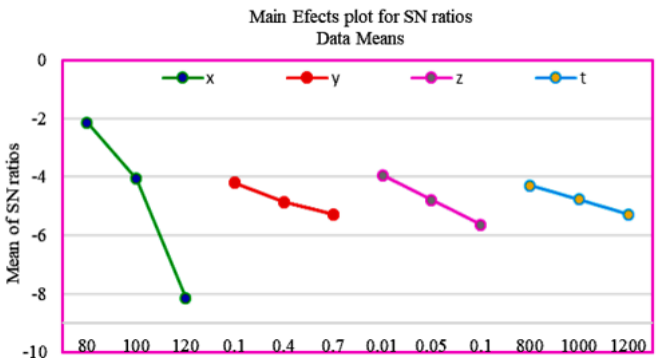

Figure 4. Main effects plot for S/N ratios

4.5 Analysis of mean

The average values of GRG for every level of every design variable are listed in Table 8. In this table, the delta values were calculated as the values of Level 1 minus Level 3. The rank values were determined for the maximum of the delta values. The maximum delta values determined the influences of the design variables. Variable (x) significantly affected the acceleration and CF, followed by variable (z), variable (t), and finally, variable (y). The data in Table 8 created the curves in Figure 5. Similar to Table 7, in this Fig, the effects of the design variables were determined by the slope of the graph; the larger the slope, the stronger the influence of those variables on the GRG values or the acceleration and CF. As such, variable (x) showed the most significant influence on the acceleration and the CF of the slider and crank, followed by variable (z), variable (t), and finally, variable (y). The high peaks on the plot indicate the optimal levels of the design variables, meaning that the optimal level was Level 1 for the design variables obtained. The problem consistent with previous studies [2, 5-7, 23, 24]. This means the acceleration and the VF depend on the crank length, clearance size, coefficient friction and input velocity.

Table 8. Mean values of GRG

Level	x	y	z	t
1	0.7861	0.6422	0.6669	0.6424
2	0.6310	0.5961	0.5998	0.6033
3	0.3931	0.5719	0.5435	0.5645
Delta	0.3929	0.0704	0.1234	0.0779
Rank	1	4	2	3

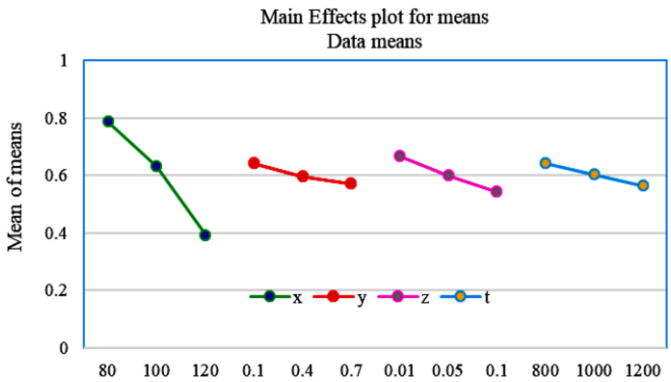

Figure 5. The graph of main effects plot for mean

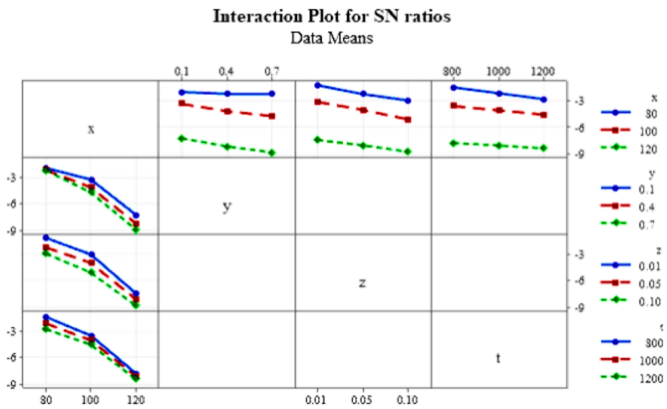

Figure 6. Interaction plot for S/N

4.6 Analysis of interaction

In order to verify variable interactions, the interaction analysis tool in Minitab was used to estimate the interaction

level between the variables. The outputs highlighted in Figure 6 verify that variables (x) and (t) significantly affect the S/N of GRG, while the variables (y) and (z) have slight effects on the S/N of GRG. The variables (x) and (t) significantly affect the acceleration and CF, as depicted on the interaction plots as non-parallel lines, while variables (y) and (z) slightly affect the acceleration and CF, as illustrated on the interaction plots as parallel lines. The problem consistent with previous studies [2, 5-7, 23, 24]. This means the acceleration and the CF depend on the crank length, clearance size, coefficient friction and input velocity.

Similarly, Figure 7 highlights that variables (x) and (t) significantly affect the mean values for GRG, while the variables (y) and variable (z) slightly affect the mean values for GRG. The variables (x) and (t) significantly affect the acceleration and the CF, as depicted on the interaction plots as non-parallel lines. In contrast, the variables (y) and (z) slightly affect the acceleration and the CF and are shown on the interaction plots as parallel lines. The problem consistent with previous studies [2, 5-7, 23, 24]. This means the acceleration and the CF depend on the crank length, clearance size, coefficient friction and input velocity.

4.7 Analysis of variance

The effect of the variables on acceleration and CF was confirmed by GRA based on S/N analysis as well as by analysis of variance (ANOVA), the results of which are presented in Table 9. The contribution percent of (x) is 83.32%, (y) is 2.72%, (z) is 8.11%, (t) is 3.23%, (x*y) is 0.59%, (x*z) is 1.04%, (x*t) is 0.75%, and the error is 0.23%. The P-values equal to zero reveal that variable (x) has the strongest influence, followed by variable (z), variable (t), and finally, variable (y). These results are also true for S/N. The problem consistent with previous studies [2, 5-7, 23, 24]. This means the acceleration and the CF depend on the crank length, clearance size, coefficient friction and input velocity.

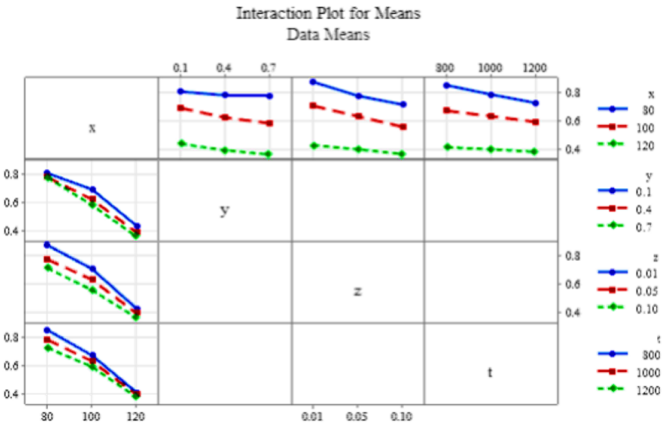

Figure 7. Interaction plot for means

Table 9. Analysis of variance

Source	DF	Seq SS	Contribution	Adj SS	Adj MS	F-Value	P-Value
x	2	0.704990	83.32%	0.704990	0.352495	1074.79	0.000
y	2	0.023005	2.72%	0.023005	0.011503	35.07	0.000
z	2	0.068661	8.11%	0.068661	0.034330	104.68	0.000
t	2	0.027308	3.23%	0.027308	0.013654	41.63	0.000
x*y	4	0.004968	0.59%	0.004968	0.001742	5.79	0.042
x*z	4	0.008842	1.04%	0.008842	0.002210	6.74	0.021
x*t	4	0.006370	0.75%	0.006370	0.001593	4.86	0.043
Error	6	0.001968	0.23%	0.001968	0.000328		
Total	26	0.846112	100.00%				

The outcomes of R-sq, R-sq (adj), and R-sq (pred) are 99.77%, 98.99%, and 97.29%, respectively, as presented in Table 10.

Table 10. Model summary

S	R-sq	R-sq (adj)	PRESS	R-sq (pred)
0.0181098	99.77%	98.99%	0.0398478	97.29%

$$\mu_{GRG} = GRG_m + \sum_{i=1}^{q}\left(GRG_{Oi} - GRG_m\right) = x1 + y1 + z1 + t1 - 3GRG_m$$

$$= 0.7861 + 0.6422 + 0.6669 + 0.6424 - 3^{*}0.6034 = 0.9273$$

At α=0.05, fe=6, $F_{0.05}(1,6)$=5.9874 [49], Ve=0.000328, R=20, Re=1, n=27,

$$CI_{CE} = \pm\sqrt{5.9874 \times 0.000328 \times \left(\frac{1}{\frac{27}{1+20}} + 1\right)} = \pm 0.06$$

$$0.86728 < \mu_{\text{confirmation}} < 0.98728$$

The optimal and forecasted values of GRG are 0.967 and 0.9273, respectively, with a very low error of 3.97%. These results clearly indicate that the variables significantly affect the CF and acceleration. The predicted and optimal outcomes determined by the GRA based on the Taguchi method have an error of less than 4%.

4.8 Results of TOPSIS

In order to confirm the optimal results of the GRA, TOPSIS was also utilized in this investigation. The values of n_{ij}, were calculated by inserting the acceleration and CF values listed in Table 3 in Eq. (18). Next, Eq. (19), Eq. (22), Eq. (23), and Eq. (24) were applied to determine the values of $v_{ij}, S_i+, S_i-,$ and CC_i respectively. All of the TOPSIS outcomes are presented in Table 11. The maximum value of CC_i indicates that the first case was optimal and ranked 1. The problem consistent with previous studies [2, 5-7, 23, 24]. This means the acceleration and the CF depend on the crank length, clearance size, coefficient friction and input velocity.

4.9 Results of SAW

In addition to the TOPSIS method, the SAW method was

also applied to verify the results of GRA. Following the SAW method, the values of n_{ij} were obtained by inserting the acceleration and CF values in Table 3 in Eq. (25). Next, Eq. (26) was applied to determine the values of v_i. The results of this method are presented in Table 12. The maximum value of v_i was obtained for the first case, pointed out that the 1st case was the optimum case. The problem consistent with previous studies [2, 5-7, 23, 24]. This means the acceleration and the CF depend on the crank length, clearance size, coefficient friction and input velocity.

Table 11. Results of the TOPSIS method

Experiment No.	n_{ij}		b_{ij}		S_{i^+}	S_{i^-}	CC_i	Rank
	D_i	S_t	D_i	S_t				
1	0.0767	0.0535	0.0446	0.0224	0.0056	0.1884	0.9714	1
2	0.1198	0.0698	0.0697	0.0292	0.0280	0.1689	0.8580	5
3	0.1725	0.0777	0.1003	0.0325	0.0579	0.1525	0.7248	11
4	0.0964	0.0633	0.0561	0.0265	0.0150	0.1784	0.9223	2
5	0.1469	0.0700	0.0854	0.0293	0.0427	0.1614	0.7909	7
6	0.1659	0.0422	0.0965	0.0177	0.0519	0.1677	0.7638	9
7	0.1187	0.0658	0.0690	0.0276	0.0267	0.1707	0.8647	4
8	0.1283	0.0402	0.0746	0.0168	0.0300	0.1774	0.8553	6
9	0.1878	0.0468	0.1092	0.0196	0.0647	0.1618	0.7144	12
10	0.1230	0.0491	0.0715	0.0206	0.0272	0.1755	0.8658	3
11	0.1566	0.0815	0.0911	0.0341	0.0496	0.1546	0.7571	10
12	0.1954	0.1225	0.1136	0.0513	0.0771	0.1303	0.6281	17
13	0.1472	0.0855	0.0856	0.0358	0.0452	0.1555	0.7750	8
14	0.1788	0.1189	0.1040	0.0498	0.0679	0.1351	0.6655	15
15	0.1862	0.1240	0.1083	0.0519	0.0727	0.1315	0.6440	16
16	0.1691	0.1173	0.0983	0.0491	0.0627	0.1380	0.6877	14
17	0.1650	0.1167	0.0959	0.0489	0.0605	0.1392	0.6970	13
18	0.2055	0.1598	0.1195	0.0669	0.0901	0.1136	0.5578	18
19	0.2195	0.1833	0.1276	0.0767	0.1024	0.1018	0.4985	19
20	0.2364	0.2349	0.1375	0.0983	0.1236	0.0784	0.3882	20
21	0.2597	0.3006	0.1510	0.1258	0.1523	0.0490	0.2434	22
22	0.2415	0.2552	0.1404	0.1068	0.1315	0.0695	0.3457	21
23	0.2579	0.3108	0.1499	0.1301	0.1547	0.0449	0.2249	23
24	0.2503	0.3427	0.1455	0.1435	0.1619	0.0327	0.1682	25
25	0.2642	0.3203	0.1536	0.1341	0.1601	0.0406	0.2023	24
26	0.2473	0.3446	0.1438	0.1442	0.1615	0.0326	0.1679	26
27	0.2677	0.4171	0.1556	0.1746	0.1929	0.0000	0.0000	27

Table 12. Results of the SAW method

Experiment No.	n_{ij}		v_i	Rank
	D_i	S_t		
1	1.00000	0.75186	0.89613	1
2	0.63996	0.57613	0.61324	7
3	0.44442	0.51729	0.47492	12
4	0.79500	0.63450	0.72782	3
5	0.52210	0.57394	0.54380	9
6	0.46215	0.95316	0.66769	5
7	0.64580	0.61056	0.63105	6
8	0.59772	1.00000	0.76611	2
9	0.40819	0.85952	0.59712	8
10	0.62326	0.81855	0.70501	4
11	0.48951	0.49315	0.49103	11
12	0.39246	0.32796	0.36546	17
13	0.52099	0.47020	0.49973	10
14	0.42874	0.33802	0.39077	15
15	0.41172	0.32415	0.37506	16
16	0.45352	0.34264	0.40710	14
17	0.46478	0.34439	0.41438	13
18	0.37316	0.25152	0.32224	18
19	0.34924	0.21928	0.29484	19
20	0.32428	0.17108	0.26015	20
21	0.29523	0.13371	0.22762	23
22	0.31748	0.15749	0.25051	21
23	0.29735	0.12933	0.22702	25
24	0.30637	0.11726	0.22721	24
25	0.29023	0.12550	0.22127	26
26	0.31002	0.11663	0.22907	22
27	0.28644	0.09635	0.20687	27

4.10 Results of WASPAS

In order to determine that the 1st case is the optimum case-as indicated by the GRA-the WASPAS method was also applied to increase the reliability. Following this method, the n_{ij} were obtained by substituting the acceleration and CF values in Table 3 in Eq. (25). Next, the values of $v_{ij}, Q_i, P_i,$ and A_i were determined using Eqs. (28)-(31), respectively. The results of this method were listed in Table 13. The maximum value of A_i was obtained for the first case, indicating that it was the optimal case. The problem consistent with previous studies [2, 5-7, 23, 24]. This means the acceleration and the CF depend on the crank length, clearance size, coefficient friction and input velocity.

The limitation of the proposed method is that it has not been confirmed by experimental results because it will cost a lot as well as not being able to establish a mathematical model and solve the mathematical model using a programming language because this method is quite complicated.

4.11 Optimal results

For the optimal case, the graph of the slider's velocity is provided in Figure 8. In the figure, the slider's velocity with a clearance size of all clearance joints equal to 0.1 mm and an ideal clearance size of zero are plotted on the same axis. A plot of the acceleration of the slider with slight vibrations is presented in Figure 9. Plots of the CF in the RCJ, two spherical clearance joints, and a translation joint are shown in Figures

10-13, respectively. The vibrations are stronger than those with ideal joints due to the journal and ball impact on the bearing and socket in the joints with clearance. From the plots of the acceleration of the slider and the CF in the revolute, spherical joints with clearance, and translation joints, the motion of the journal and ball in the bearing and socket has three types of motion: free light, contact, and impact. These phenomena were also described in references [2, 5-7, 23, 24]. However, these oscillations are stable based on the optimization by GRA based on the Taguchi method; the optimal results were also confirmed by the TOPSIS, SAW, and WASPAS methods.

Table 13. Results of the WASPAS method

Experiment No.	n_{ij}		v_{ij}		Q_i	P_i	A_i	Rank
	D_i	S_t	D_i	S_t				
1	1.0000	0.7519	0.5814	0.3147	0.8961	0.4497	0.8515	1
2	0.6400	0.5761	0.3721	0.2412	0.6132	0.3103	0.5830	7
3	0.4444	0.5173	0.2584	0.2165	0.4749	0.2400	0.4514	12
4	0.7950	0.6345	0.4622	0.2656	0.7278	0.3665	0.6917	3
5	0.5221	0.5739	0.3036	0.2402	0.5438	0.2752	0.5169	9
6	0.4622	0.9532	0.2687	0.3990	0.6677	0.3171	0.6326	5
7	0.6458	0.6106	0.3755	0.2556	0.6310	0.3196	0.5999	6
8	0.5977	1.0000	0.3475	0.4186	0.7661	0.3757	0.7271	2
9	0.4082	0.8595	0.2373	0.3598	0.5971	0.2825	0.5657	8
10	0.6233	0.8185	0.3624	0.3426	0.7050	0.3540	0.6699	4
11	0.4895	0.4931	0.2846	0.2064	0.4910	0.2488	0.4668	11
12	0.3925	0.3280	0.2282	0.1373	0.3655	0.1845	0.3474	17
13	0.5210	0.4702	0.3029	0.1968	0.4997	0.2529	0.4750	10
14	0.4287	0.3380	0.2493	0.1415	0.3908	0.1967	0.3714	15
15	0.4117	0.3241	0.2394	0.1357	0.3751	0.1887	0.3564	16
16	0.4535	0.3426	0.2637	0.1434	0.4071	0.2044	0.3868	14
17	0.4648	0.3444	0.2702	0.1442	0.4144	0.2077	0.3937	13
18	0.3732	0.2515	0.2170	0.1053	0.3222	0.1603	0.3060	18
19	0.3492	0.2193	0.2030	0.0918	0.2948	0.1456	0.2799	19
20	0.3243	0.1711	0.1885	0.0716	0.2602	0.1257	0.2467	20
21	0.2952	0.1337	0.1716	0.0560	0.2276	0.1074	0.2156	23
22	0.3175	0.1575	0.1846	0.0659	0.2505	0.1200	0.2375	21
23	0.2973	0.1293	0.1729	0.0541	0.2270	0.1063	0.2149	24
24	0.3064	0.1173	0.1781	0.0491	0.2272	0.1038	0.2149	25
25	0.2902	0.1255	0.1687	0.0525	0.2213	0.1035	0.2095	26
26	0.3100	0.1166	0.1803	0.0488	0.2291	0.1043	0.2166	22
27	0.2864	0.0964	0.1665	0.0403	0.2069	0.0920	0.1954	27

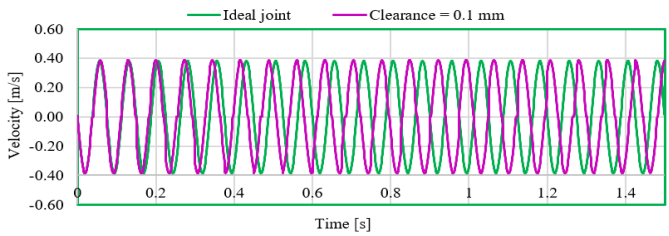

Figure 8. Velocity of the slider

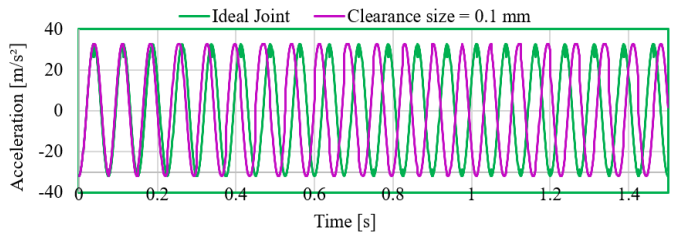

Figure 9. Acceleration of the slider

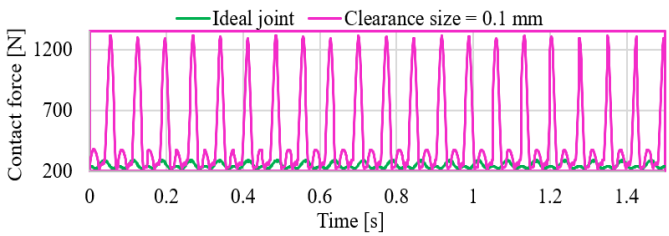

Figure 10. Contact force of the revolute clearance joint

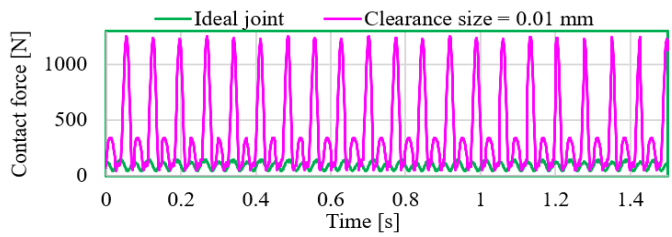

Figure 11. Contact force of the 1st spherical joint

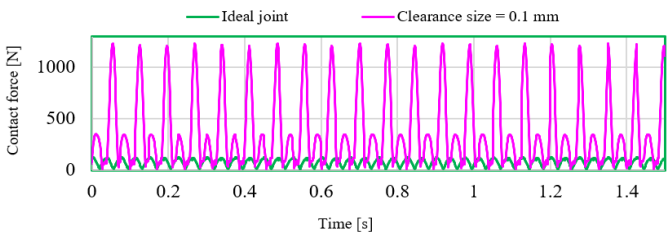

Figure 12. Contact force of the 2nd spherical joint

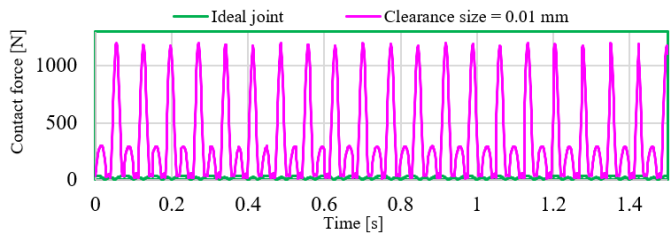

Figure 13. Total contact force of the translation joint

5. CONCLUSION

Based on the results of the Runge-Kutta 4 rigid dynamics model in ANSYS, the design variables significantly affected on the acceleration and the CF in the RCJ and imperfect spherical and translation joints. The output of the GRA based on the Taguchi method confirmed that the crank length and driving speed significantly affect the acceleration of the slider and CF in the clearance joints. In contrast, clearance size and friction slightly influence the acceleration and CF. Outcomes of the interaction analysis, ANOVA, and regression analysis also confirmed the model outcomes. In addition, the optimal values are compared with predicted values; all of the outputs are in good agreement with the GRA based on the Taguchi method, with an error of less than 4%. The optimal values obtained for the acceleration of the slider and the CF were 32.72 m/s^2 and 1.3452 kN, respectively. The TOPSIS, SAW, and WASPAS methods also verified the optimal values. All four methods provide outputs that identify the first case as optimal; the combination design includes a crank length of 80 mm, a clearance size of 0.1 mm, a friction coefficient of 0.01, and an input velocity of 800 rpm. To reduce vibration in the mechanical system, acceleration and force must be limited. The proposed method also achieves a reliable assessment result and is confirmed by the decision-making criteria. The deviation between the predicted value and the optimal value is very low. It indicated that the results of the proposed optimization method are reliable. The factors that affected on the vibration of the mechanical system are the selected design variables. The limitation of this study is that the optimal case is within the limit of 27 cases. Compared to other methods, the optimal level of design variables and optimal cases are outside the 27 cases. That means it cannot be ruled out that the optimal case is something else. Because of the limitations of the proposed method in the analysis and discussion section. Therefore, future research will focus on theoretical and experimental research to confirm the results of ANSYS simulation analysis and the results of the optimization methods proposed.

ACKNOWLEDGEMENTS

This work was financially supported by PetroVietnam University (Grant No.: GV2208).

REFERENCES

[1] Chen, X.L., Gao, S. (2022). Dynamic response and dynamic accuracy reliability of planar mechanism with multiple lubricated clearances. Multibody System Dynamics, 57: 1-23. https://doi.org/10.1007/s11044-022-09853-w

[2] Xiao, L.J., Yan, F.P., Chen, T.X., Zhang, S.S., Jiang, S. (2022). Study on nonlinear dynamics of rigid-flexible coupling multi-link mechanism considering various kinds of clearances. Nonlinear Dynamics, 111(4): 3279-3306. https://doi.org/10.1007/s11071-022-08033-x

[3] Tan, H.Y., Li, L., Huang, Q., Jiang, Z.D., Li, Q.X., Zhang, Y.M., Yu, D.L. (2023). Influence of two kinds of clearance joints on the dynamics of planar mechanical system based on a modified contact force model. Scientific Reports, 13(1): 20569. https://doi.org/10.1038/s41598-023-47315-1

[4] Zhang, L., Fang, Y.N., Bai, G.H., Tao, J.Y. (2023). Dynamic investigations on the wear behavior of a 3D revolute joint considering time-varying contact stiffness: Simulation and experiment. Chinese Journal of Mechanical Engineering, 36(1): 1-17. https://doi.org/10.1186/s10033-023-00949-8

[5] Du, Y.J., Jiao, F.Z., Wang, P., Liu, F., Li, L. (2024). Nonsmooth dynamic modeling and simulation of spatial mechanisms with frictional translational clearance joints. Journal of Physics: Conference Series, 2746(1): 1-8. https://doi.org/10.1088/1742-6596/2746/1/012013

[6] Guo, J.N., Wang, Y.Z., Zhang, X.W., Cao, S., Liu, Z.S. (2024). Dynamic characteristic of rudder loop with rough revolute joint clearance. Nonlinear Dynamics, 112(5): 3179-3194. https://doi.org/10.1007/s11071-023-09131-0

[7] Li, S.Y., Zheng, Y.F., Wu, H.W., Zhang, J.Y., Ohsaki, M., Yang, C., Luo, Y.Z. (2024). Dynamics analysis of deployment process of the Bennett linkage with revolute clearance joints. Nonlinear Dynamics, 112(13): 10911-10935. https://doi.org/10.1007/s11071-024-09603-x

[8] Liu, S., Gu, B., Yu, H.D., Hu, C.X. (2024). Tolerance design of revolute clearance joints for aero-engine planar maneuvering mechanism by uncertain dynamic performance evaluation. International Journal of Mechanics and Materials in Design. https://doi.org/10.1007/s10999-024-09717-5

[9] Liu, Z., Zhang, H., Meng, L., Sun, Y., Luo, S.H., Zhou, L.C., Li, P. (2024). A new kinematic model for revolute clearance joints with noncircular bushing and pin in planar multibody systems. Nonlinear Dynamics, 112: 12965-12993. https://doi.org/10.1007/s11071-024-09725-2

[10] López-Lombardero, M., Cuadrado, J., Cabello, M., Martinez, F., Dopico, D., López-Varela, A. (2024). A multibody-dynamics based method for the estimation of wear evolution in the revolute joints of mechanisms that considers link flexibility. Mechanism and Machine Theory, 194: 105583. https://doi.org/10.1016/j.mechmachtheory.2024.105583

[11] Sheng, Y.C., Chen, X.L. (2024). Dynamics behavior analysis of spatial parallel coordinate measuring mechanism with spherical clearance joints. Mechanics & Industry, 25: 5. https://doi.org/10.1051/meca/2023044

[12] Wang, X., Liu, G., Ma, S., Tong, R. (2019). Study on dynamic responses of planar multibody systems with dry revolute clearance joint: numerical and experimental approaches. Journal of Sound and Vibration, 438: 116-138. https://doi.org/10.1016/j.jsv.2018.08.052

[13] Chen, Y., Wu, K., Wu, X., Sun, Y., Zhong, T. (2021). Kinematic accuracy and nonlinear dynamics of a flexible slider-crank mechanism with multiple clearance joints. European Journal of Mechanics-A/Solids, 88: 104277. https://doi.org/10.1016/j.euromechsol.2021.104277

[14] Li, Y., Yang, Y., Li, M., Liu, Y., Huang, Y. (2022). Dynamics analysis and wear prediction of rigid-flexible coupling deployable solar array system with clearance joints considering solid lubrication. Mechanical Systems and Signal Processing, 162: 108059. https://doi.org/10.1016/j.ymssp.2021.108059

[15] Chen, Z.Q., Qian, L.F., Chen, G.S., Niu, S.C., Yin, Q., Yue, C.C. (2022). Dynamics of luffing motion of a hydraulically driven shell manipulator with revolute clearance joints. Defence Technology, 18(4): 689-708.

https://doi.org/10.1016/j.dt.2021.02.004
[16] Chen, X., Guo, J. (2020). Effects of spherical clearance joint on dynamics of redundant driving spatial parallel mechanism. Robotica, 39(6): 1064-1080. https://doi.org/10.1017/s0263574720000909
[17] Guo, F., Cheng, G., Wang, S., Li, J. (2022). Rigid–Flexible coupling dynamics analysis with joint clearance for a 5-DOF hybrid polishing robot. Robotica, 40(7): 2168-2188. https://doi.org/10.1017/s0263574721001594
[18] Hou, Y.L., Deng, Y.J., Zeng, D.X. (2021). Dynamic modelling and properties analysis of 3RSR parallel mechanism considering spherical joint clearance and wear. Journal of Central South University, 28(3): 712-727. https://doi.org/10.1007/s11771-021-4640-y
[19] Ordiz, M., Cuadrado, J., Cabello, M., Retolaza, I., Martinez, F., Dopico, D. (2021). Prediction of fatigue life in multibody systems considering the increase of dynamic loads due to wear in clearances. Mechanism and Machine Theory, 160: 104293. https://doi.org/10.1016/j.mechmachtheory.2021.104293
[20] Wang, X., Rui, X. (2021). Dynamics modeling and simulation of tracked armored vehicle with planar clearance trunnion-bearing revolute joint. Journal of Mechanical Science and Technology, 35(6): 2285-2302. https://doi.org/10.1007/s12206-021-0502-7
[21] Wu, X., Sun, Y., Wang, Y., Chen, Y. (2021). Correlation dimension and bifurcation analysis for the planar slider-crank mechanism with multiple clearance joints. Multibody System Dynamics, 52, 95-116. https://doi.org/10.1007/s11044-020-09769-3
[22] Huynh, N.T., Hoang, C.R., Tran, T.K., Van Hoai, L.E. (2021). Analysis of rigid and flexible dynamics of a space-slider-crank mechanism based on finite element method. Journal of Science and Technology-IUH, 50(2): 292-302. https://doi.org/10.46242/jst-iuh.v50i08.981
[23] Wang, C.N., Le, T.D.M., Huynh, N.T. (2023). Optimal rigid-flexible dynamic of space slider-crank mechanism with clearance joints. Sādhanā, 48(2): 44. https://doi.org/10.1007/s12046-023-02085-4
[24] Rodrigues da Silva, M., Marques, F., Tavares da Silva, M., Flores, P. (2022). A comparison of spherical joint models in the dynamic analysis of rigid mechanical systems: Ideal, dry, hydrodynamic and bushing approaches. Multibody System Dynamics, 56(3): 221-266. https://doi.org/10.1007/s11044-022-09843-y
[25] Chen, X., Jia, Y. (2022). Dynamic modeling and responses investigation of spatial parallel robot considering lubricated spherical joint. European Journal of Mechanics-A/Solids, 92: 104458. https://doi.org/10.1016/j.euromechsol.2021.104458
[26] Hao, J.Y., Long, C.X. (2021). Dynamic response analysis for multi-degrees-of-freedom parallel mechanisms with various types of three-dimensional clearance joints. International Journal of Advanced Robotic Systems, 18(3). https://doi.org/10.1177/17298814211017716
[27] Ikeagwuani, C.C., Agunwamba, J.C., Nwankwo, C.M., Eneh, M. (2021). Additives optimization for expansive soil subgrade modification based on Taguchi grey relational analysis. International Journal of Pavement Research and Technology, 14: 138-152. https://doi.org/10.1007/s42947-020-1119-4
[28] Miç, P., Antmen, Z.F. (2021). A decision-making model based on TOPSIS, WASPAS, and MULTIMOORA methods for university location selection problem. Sage Open, 11(3): 21582440211040115. https://doi.org/10.1177/21582440211040115
[29] Cicioğlu, M. (2021). Multi-criteria handover management using entropy-based SAW method for SDN-based 5G small cells. Wireless Networks, 27(4): 2947-2959. https://doi.org/10.1007/s11276-021-02625-y
[30] Bai, Z.F., Ning, Z.Y., Zhou, J.S. (2022). Study on wear characteristics of revolute clearance joints in mechanical systems. Micromachines (Basel), 13(7): 1018. https://doi.org/10.3390/mi13071018
[31] Bai, Z.F., Xu, F.S., Zhao, J.J. (2021). Numerical and experimental study on dynamics of the planar mechanical system considering two revolute clearance joints. International Journal of Mechanical System Dynamics, 1(2): 256-266. https://doi.org/10.1002/msd2.12022
[32] Song, N.N., Peng, H.J., Xu, X.M., Wang, G. (2020). Modeling and simulation of a planar rigid multibody system with multiple revolute clearance joints based on variational inequality. Mechanism and Machine Theory, 154. https://doi.org/10.1016/j.mechmachtheory.2020.104053
[33] Chen, Y., Feng, J., Peng, X., Sun, Y., He, Q., Yu, C.T. (2020). An approach for dynamic analysis of planar multibody systems with revolute clearance joints. Engineering with Computers, 37(3): 2159-2172. https://doi.org/10.1007/s00366-020-00935-x
[34] Bai, Z.F., Jiang, X., Li, J.Y., Zhao, J.J., Zhao, Y. (2020). Dynamic analysis of mechanical system considering radial and axial clearances in 3D revolute clearance joints. Journal of Vibration and Control, 27(15-16): 1893-1909. https://doi.org/10.1177/1077546320950517
[35] Chen, X.L., Jiang, S.Y. (2020). Dynamic response and chaos in planar multi-link mechanism considering revolute clearances. Archive of Applied Mechanics, 90: 1919-1941. https://doi.org/10.1007/s00419-020-01704-4
[36] Shanmugasundar, G., Sapkota, G., Čep, R., Kalita, K. (2022). Application of MEREC in multi-criteria selection of optimal spray-painting robot. Processes, 10(6): 1172. https://doi.org/10.3390/pr10061172
[37] Ecer, F., Aycin, E. (2023). Novel comprehensive MEREC weighting-based score aggregation model for measuring innovation performance: The case of G7 countries. Informatica, 34(1): 53-83. https://doi.org/10.15388/22-infor494
[38] Mishra, A.R., Saha, A., Rani, P., Hezam, I.M., Shrivastava, R., Smarandache, F. (2022). An integrated decision support framework using single-valued-MEREC-MULTIMOORA for low carbon tourism strategy assessment. IEEE Access, 10: 24411-24432. https://doi.org/10.1109/access.2022.3155171
[39] Banik, B., Alam, S., Chakraborty, A. (2023). Comparative study between GRA and MEREC technique on an agricultural-based MCGDM problem in pentagonal neutrosophic environment. International Journal of Environmental Science and Technology, 20(12): 13091-13106. https://doi.org/10.1007/s13762-023-04768-1
[40] Silva, N.F., dos Santos, M., Gomes, C.F.S., de Andrade, L.P. (2023). An integrated CRITIC and Grey Relational Analysis approach for investment portfolio selection. Decision Analytics Journal, 8: 100285. https://doi.org/10.1016/j.dajour.2023.100285

[41] Sheth, M., Gajjar, K., Jain, A., Shah, V., Patel, H., Chaudhari, R., Vora, J. (2021). Multi-objective optimization of Inconel 718 using Combined approach of Taguchi—Grey relational analysis. In Advances in Mechanical Engineering: Select Proceedings of ICAME 2020, 229-235. https://doi.org/10.1007/978-981-15-3639-7_27

[42] Awale, A., Inamdar, K. (2020). Multi-objective optimization of high-speed turning parameters for hardened AISI S7 tool steel using grey relational analysis. Journal of the Brazilian Society of Mechanical Sciences and Engineering, 42(7): 356. https://doi.org/10.1007/s40430-020-02433-z

[43] Asiltürk, I., Neşeli, S., Ince, M.A. (2016). Optimisation of parameters affecting surface roughness of Co28Cr6Mo medical material during CNC lathe machining by using the Taguchi and RSM methods. Measurement, 78: 120-128. https://doi.org/10.1016/j.measurement.2015.09.052

[44] Sarıkaya, M., Güllü, A. (2015). Multi-response optimization of minimum quantity lubrication parameters using Taguchi-based grey relational analysis in turning of difficult-to-cut alloy Haynes 25. Journal of Cleaner Production, 91: 347-357. https://doi.org/10.1016/j.jclepro.2014.12.020

[45] Deepanraj, B., Sivasubramanian, V., Jayaraj, S. (2017). Multi-response optimization of process parameters in biogas production from food waste using Taguchi–Grey relational analysis. Energy Conversion and Management, 141: 429-438. https://doi.org/10.1016/j.enconman.2016.12.013

[46] Sheng, D.Y. (2020). Design optimization of a single-strand tundish based on CFD-Taguchi-grey relational analysis combined method. Metals, 10(11): 1539. https://doi.org/10.3390/met10111539

[47] Agboola, O.O., Ikubanni, P.P., Adeleke, A.A., Adediran, A.A., Adesina, O.S., Aliyu, S.J., Olabamiji, T.S. (2020). Optimization of heat treatment parameters of medium carbon steel quenched in different media using Taguchi method and grey relational analysis. Heliyon, 6(7): e04444. https://doi.org/10.1016/j.heliyon.2020.e04444

[48] Roy, R.K. (2010). A Primer on the Taguchi Method. Society of Manufacturing Engineers.

[49] Tuş, A., Aytaç Adalı, E. (2019). The new combination with CRITIC and WASPAS methods for the time and attendance software selection problem. Opsearch, 56: 528-538. https://doi.org/10.1007/s12597-019-00371-6

[50] Niranjan, T., Singaravel, B., Raju, S.S. (2022). Optimization of hole quality parameters using TOPSIS method in drilling of GFRP composite. Materials Today: Proceedings, 62: 2109-2114. https://doi.org/10.1016/j.matpr.2022.03.042

[51] Prabhuram, T., Singh, S.P., Durairaj, J.I., Elilraja, D., Das, M. C., Sunderraj, D.A.J. (2022). Optimization of operation parameters in machining of functionally graded metal matrix composite using TOPSIS. Materials Today: Proceedings, 62: 429-433. https://doi.org/10.1016/j.matpr.2022.03.562

[52] Meshram, S.G., Alvandi, E., Meshram, C., Kahya, E., Fadhil Al-Quraishi, A.M. (2020). Application of SAW and TOPSIS in prioritizing watersheds. Water Resources Management, 34: 715-732. https://doi.org/10.1007/s11269-019-02470-x

[53] Ccatamayo-Barrios, J.H., Huamán-Romaní, Y.L., Seminario-Morales, M.V., Flores-Castillo, M.M., Gutiérrez-Gómez, E., Carrillo-De la cruz, L.K., de la Cruz-Girón, K.A. (2023). Comparative analysis of AHP and TOPSIS multi-criteria decision-making methods for mining method selection. Mathematical Modelling of Engineering Problems, 10(5): 1665-1674. https://doi.org/10.18280/mmep.100516

[54] Khotimah, B.K., Anamisa, D.R., Kustiyahningsih, Y., Fauziah, A.N., Setiawan, E. (2024). Enhancing small and medium enterprises: A hybrid clustering and AHP-TOPSIS decision support framework. Ingénierie des Systèmes d'Information, 29(1): 313-321. https://doi.org/10.18280/isi.290131

[55] Rudnik, K., Bocewicz, G., Kucińska-Landwójtowicz, A., Czabak-Górska, I.D. (2021). Ordered fuzzy WASPAS method for selection of improvement projects. Expert Systems with Applications, 169: 114471. https://doi.org/10.1016/j.eswa.2020.114471

[56] Yücenur, G.N., Ipekçi, A. (2021). SWARA/WASPAS methods for a marine current energy plant location selection problem. Renewable Energy, 163: 1287-1298. https://doi.org/10.1016/j.renene.2020.08.131